

Modified Synchronous Reluctance Motor for Electric Vehicle Applications

Busireddy Hemanth Kumar^{1*}, Deepak Prakash Kadam², Saka Rajitha³, Prabhu Sundaramoorthy⁴, T. Panchalaiah⁵ and Kavali Janardhan⁶

¹Assistant Professor, Department of EEE, Sree Vidyanikethan Engineering College, hemub09@gmail.com

²Associate professor, Department of EEE, MET Institute of engineering, dpkadam@gmail.com

³Assistant Professor(C), JNTU-GV College of Engineering Vizianagaram, rajithasaka@gmail.com

⁴Associate Professor, Department of EEE, Sree Vidyanikethan Engineering College, prabhutajmahal6@gmail.com

⁵Assistant Professor, Department of EEE, Sree Vidyanikethan Engineering College, penchalaiah.t@vidyanikethan.edu

⁶Assistant Professor, Department of EEE, Sree Vidyanikethan Engineering College, janardhan.kavali@gmail.com

*Correspondence: Busireddy Hemanth Kumar; hemub09@gmail.com

ABSTRACT- This research article explores a comparative investigation on synchronous reluctance motor (SyRM) for electrified transportation system. The SyRM has salient features like absence of magnet, singly excited but it shrinks its application due to high torque ripple aspects. The novelty of the proposed work is the rib and flux barrier of the rotor in SyRM are modified in order to achieve low torque ripple without affecting the average torque of the motor. Analysis in the electromagnetic domain infers to enhance the sustainability and reliability of the transportation system. So, it results in the reduction of torque ripple, leads to minimize the acoustic noise. This article delivers the geometric optimization to achieve SyRM with low torque ripple. The finite elemental analysis infers the torque ripple, losses and unbalanced magnetic force for SyRM. The notched and round barrier type SyRM with one-layer results acts as superior motor among different layers and geometries. The experimental arrangement is carried out in real time vehicle and the results are obtained for different loading conditions and validated with FEA findings.

Keywords: Electric Vehicle; Layers; Power Density; Synchronous Reluctance Motor; Torque Ripple.

ARTICLE INFORMATION

Author(s): Busireddy Hemanth Kumar, Deepak Prakash Kadam, Saka Rajitha, Prabhu Sundaramoorthy, T. Panchalaiah and Kavali Janardhan;

Received: 12/09/2022; **Accepted:** 13/10/2022; **Published:** 30/10/2022;

e-ISSN: 2347-470X;

Paper Id: IJEER 1209-43;

Citation: 10.37391/IJEER.100429

Webpage-link:

<https://ijeer.forexjournal.co.in/archive/volume-10/ijeer-100429.html>



Publisher's Note: FOREX Publication stays neutral with regard to Jurisdictional claims in Published maps and institutional affiliations.

1. INTRODUCTION

As the number of electric vehicles (EVs) rises, oil reliance as well as noise and pollution levels are decreasing. High power and high energy density storage devices, along with effective power electronics-based energy conversion and electric machines, are essential components of successful technology [1]-[3]. High torque and power density, a wide speed range, high efficiency over a large torque and speed range, high dependability and robustness, among other characteristics, are essential when it comes to electric machines.

Due to its robust mechanical design, low cost, and minimal maintenance needs, the mature three-phase induction motor (IM) is acknowledged as a well-known and widely accessible structure. But this motor has a lot of issues because of how the bars are implemented on the rotor.

For many applications, including traction, permanent magnet synchronous motors (PMSMs) are the standard technology [4]. The dependability difficulties in PMSM caused by potential magnet flaws are also debatable. The difference between SyRM and its IM and PMSM equivalents is in the rotor architecture. SyRM achieves greater efficiency in the same power range with the same frame size [5], higher power density, and higher torque per ampere [6] compared to those conventional motors. It also achieves higher reliability and simpler maintenance [7], lower cost, faster dynamic response, and a greater speed range [8].

Highly efficient motor drives are provided by variable-speed drives (VSDs), particularly when operating at partial load and at high speeds [9]. As a result, SyRM are used in the industry primarily with its drive package. The emphasis on SyRM was on torque density, but subsequently, these motors have come to be seen as a very wise choice for the applications. The absence of bars in the rotor causes the iron loss to essentially be omitted, resulting in effective motor functioning [10]. Because of its advantage, the SyRM drive's payback period is so brief that replacing IM is entirely practical.

SyRM, on the other hand, has several serious disadvantages. The power factor for this technique is extremely low [11]. The saliency ratio affects the maximal power factor of SyRM. In this regard, the motor may deliver a larger power factor the higher the ratio the SyRM has. In [12], a sophisticated laminated anisotropic rotor design is put forth that can raise the saliency ratio and, as a result, enhance the power factor and torque density.

All of the advantages of the motor are retained with this tactic. However, the recent advancements made by these methods are insignificant. Significant torque ripples in SyRM are brought on by the interaction between the spatial harmonics of MMF and the rotor shape [13]. These motors' acoustic noise and high torque ripples have become a problem, which has prompted significant effort to address this flaw in both design and control aspects [14]. Some research studies [15] focus on improving the rotor structure to reduce torque ripples. Asymmetric rotor flux barriers and rotor skewing are two of the suggested design methods that can reduce torque ripples in SyRM by half and two-thirds, respectively. In terms of motor design, the permanent magnet is positioned in the auxiliary poles of the stator, and the magnet orientation guarantees that the motor produces more average torque with less cogging torque is mentioned in [16]-[18].

The confront of this paper is to springs electromagnetic analysis for various types of synchronous reluctance motors for the application of transportation and compare it in the domain of magnetic field distribution and torque characteristics. This paper investigates the electromagnetic findings, as torque ripple and average torque of SyRM for electric vehicle. The flux path and its direction are examined in various types of SyRM ensuring that less ripple content present in the torque characteristics.

2. MATHEMATICAL MODELING OF SYNCHRONOUS RELUCTANCE MOTOR

The following assumptions are considered while designing the SyRM in FEA,

- Hysteresis effects are neglected
- Time harmonic effects are absent.
- Magnetic field found in the outer periphery are neglected
- The distribution of magnetic flux density is constant with axial direction

The following equations derive the motor for the required torque in SyRM. The ratings of the SyRM motor are 2 kW, 60V, 12Nm, 1500 RPM. The dimensions of the motor to be considered are outer rotor diameter= 120mm, stack length = 50 mm and air gap = 0.3 mm. The mathematical model of Synchronous reluctance motor is used for optimum values of flux linkages and flux distribution on the motor. By using the mathematical modelling, the torque values, flux density, speed, accurate voltage of the respective motors can be found out effectively. The following expressions are considered while designing the SyRM effectively. To design the motor, finite element analysis (FEA) are executed using software packages as MagNet, MotorSolve etc. The solving technique used in the FEA is Newton Raphson.

$$\text{Flux Density, } B = \mu H, \text{ Flux, } \phi = \frac{Ni}{R} \text{ \& Reluctance, } R = \frac{l}{P} = \frac{l}{\mu A} \quad (1)$$

$$\text{Torque, } T = kD^2 L \quad (2)$$

$$\text{Power, } P_e = k_e h^2 f^2 B^2 \quad (3)$$

$$\text{Flux Density, } B_m = B_r + \mu_R \mu_o H_m \quad (4)$$

$$\text{Flux of permanent magnets } \phi = B_m A_m = B_r A_m + \mu_R \mu_o A_m H_m \quad (5)$$

$$\text{Flux Linkage of coil, } \lambda = \frac{N^2}{R} i \quad (6)$$

$$\text{Accurate Torque, } T = \frac{1}{2} i^2 \frac{dL}{d\theta} - \frac{1}{2} \phi^2 \frac{dR}{d\theta} + Ni \frac{d\phi}{d\theta} \quad (7)$$

$$\text{Inductance for air gap, } L_g = \frac{2\pi\mu_o L_{st} R_{ro}}{g + \frac{l_m}{\mu_R C_\phi}} N^2 \quad (8)$$

$$\text{Motor Constant } K_m = \frac{2NB_g L_{st} R_{ro} I}{\sqrt{I^2 (2R_{stot})}} = \frac{2NB_g L_{st} R_{ro}}{\sqrt{2\rho L_{st} N / A_{wb}}} = \frac{B_g R_{ro}}{\sqrt{\rho}} \sqrt{V_{wb}} \quad (9)$$

$$\text{Cogging Torque, } T_{cog} = -\frac{1}{2} \phi^2 \frac{dR}{d\theta} \quad \& \quad \text{Torque Ripple,}$$

$$T_{ripple} = \frac{T_{max} - T_{min}}{T_{avg}} \quad (10)$$

$$\text{Speed } N = \frac{P * 60}{2 * \pi * T} \quad \& \quad \text{Step angle} = \frac{360}{Q * N_r} \quad (11)$$

$$\text{Area of the stator, } A_s = \left[\frac{D}{2} - g \right] L \beta_s \quad (12)$$

$$\text{Flux in the stator, } \phi = B_s * A_s \quad \& \quad \text{Area of the rotor, } A_r = ((D/2) * L * \beta_r) \quad (13)$$

$$\text{Area of the Yoke, } A_y = A_r / 2.1 \quad \& \quad \text{Flux in the yoke, } \phi_y = \phi_{sc} = \phi / 2 \quad (14)$$

$$\text{Area of the air gap } A_g = \left[\frac{D}{2} - \frac{g}{2} \right] \left[\frac{\beta_r + \beta_s}{2} \right] * 75 * 10^{-6} \quad (15)$$

$$\text{Height of the stator pole and core, } h_s = \frac{D}{2} - g - \frac{D_{sh}}{2} - \frac{A_{sc}}{L} \quad \& \quad h_{sc} = \frac{A_{sc}}{L} \quad (16)$$

$$\text{Height of the rotor Pole, } h_r = \frac{D_o}{2} - C - \frac{D}{2} \quad (17)$$

$$\text{Length of the flux path in Yoke, } l_y = \pi * \left[\frac{D_o}{2} - \frac{C}{2} \right] \text{ in rotor,}$$

$$l_r = h_r + \frac{C}{2} \quad (18)$$

$$\text{The length of the flux path in stator core, } l_{sc} = \pi * \left[\frac{D}{4} - \frac{g}{2} + \frac{h_s}{2} + \frac{D_{sh}}{4} \right] \quad (19)$$

3. RESULTS

A thin rib is available in the rotor in between flux barriers provides the flux path to the rotor interior part. If the layer increases, enormously the mechanical strength of the motor gets degraded, lead to the reduction in the average torque. In this regard, the number of layers is restricted to four. And all the applications wont suits a particular layer, it depends on the power rating, required torque of the motor.

Figure 1 shows the model diagram of SyRM design having angle barrier like flux distribution with one layer.

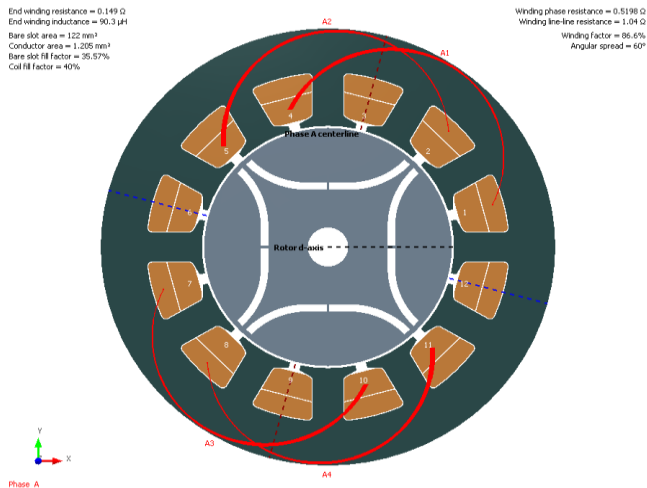


Figure 1: Model diagram of SyRM with angled barrier (1layer)

The model diagram of SyRM design having notch and angle barrier like flux distribution with one layer is shown in figure 2.

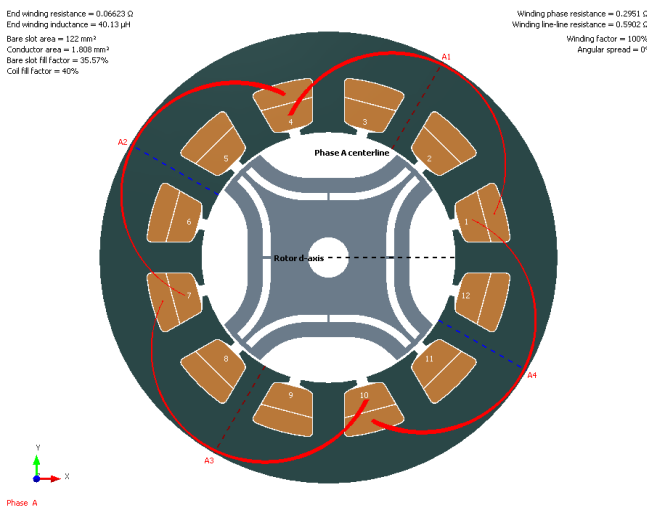


Figure 2: Model diagram of SyRM with notch and angled barrier (1layer)

Similarly Figure 3 shows the model diagram of SyRM design having round barrier like flux distribution with one layer. And the model diagram of SyRM design having notch and round barrier like flux distribution with one layer is shown in figure 4.

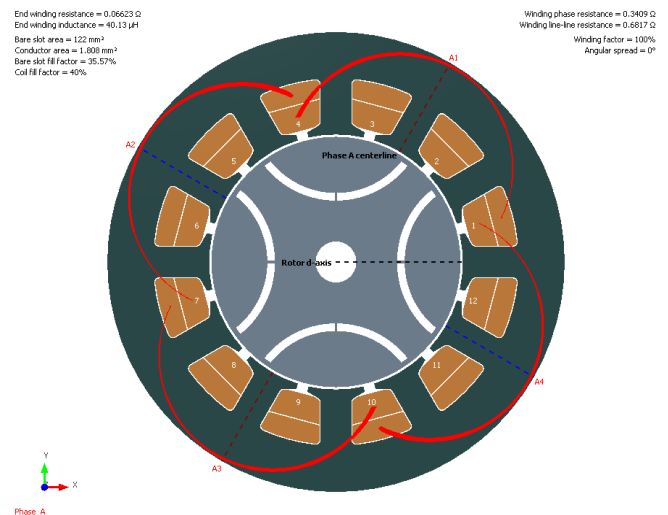


Figure 3: Model diagram of SyRM with round barrier (1layer)

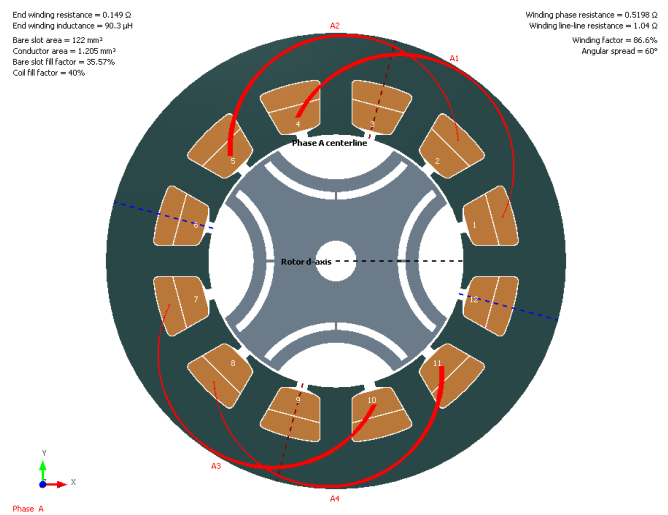
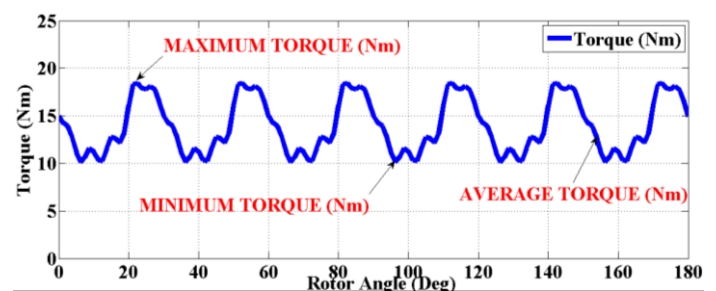
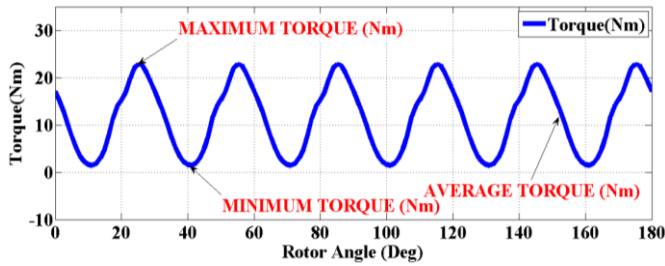


Figure 4: Model diagram of SyRM with notch and round (1layer)

Figure 5 (a) infers the torque waveform produced by the Synchronous Reluctance motor with three angled barriers with maximum, minimum and average Torque values of 18.424 Nm, 10.136 Nm and 13.968 Nm. Figure 5(b) infers the torque waveform produced by the Synchronous Reluctance motor with one angled barrier with maximum, minimum and average Torque values of 22.84 Nm, 1.426 Nm and 11.831 Nm respectively.



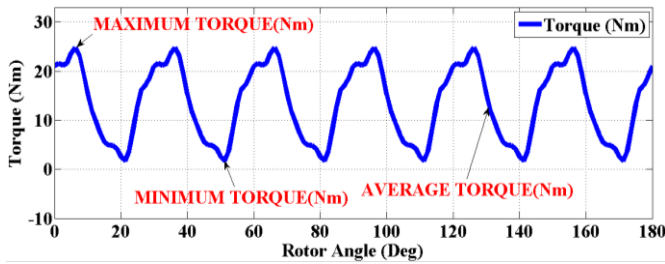
(a) 3 Layer



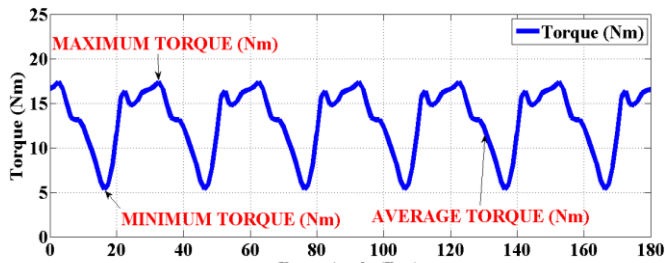
(b). 1 layer

Figure 5: Torque Waveform of SyRM with angled barrier.

Figure 6 (a) infers the torque waveform produced by the Synchronous Reluctance motor with three angled barriers with notch having maximum, minimum and average Torque values of 24.770 Nm, 1.671 Nm and 13.702 Nm. Figure 6(b) infers the Torque waveform produced by the Synchronous Reluctance motor with one angled barrier with notch having maximum, minimum and average Torque values of 17.377 Nm, 5.361 Nm and 13.055Nm respectively.



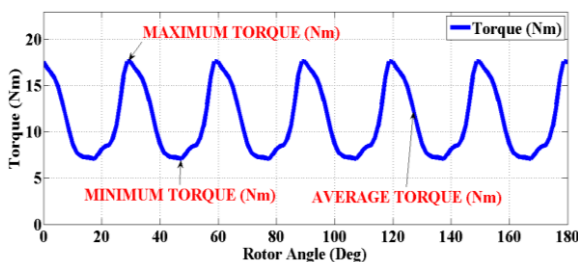
(a) 3 Layer



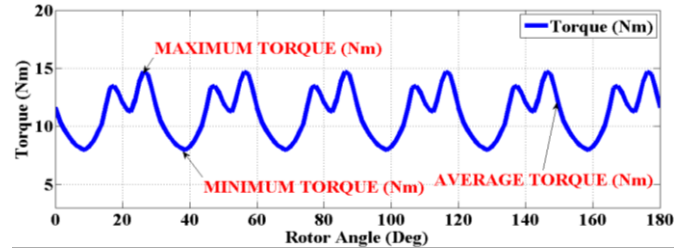
(b). 1 layer

Figure 6: Torque waveform for SyRM with notch and angled barrier

Figure 7(a) infers the torque waveform produced by the Synchronous Reluctance motor with three round barriers with maximum, minimum and average Torque values of 17.596 Nm, 7.082 Nm and 11.439 Nm and figure 7(b) infers the torque waveform produced by the Synchronous Reluctance motor with one round barrier with maximum, minimum and average torque values of 14.698 Nm, 7.970 Nm and 11.069 Nm respectively.



(a). 3 layers

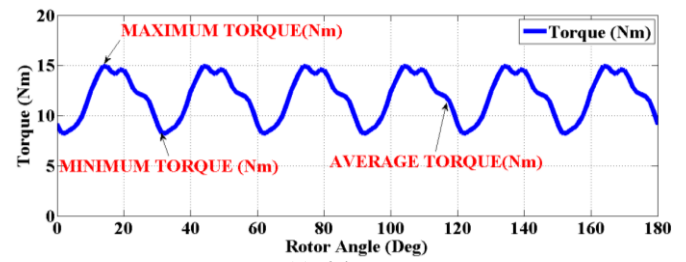


(b). 1 layer

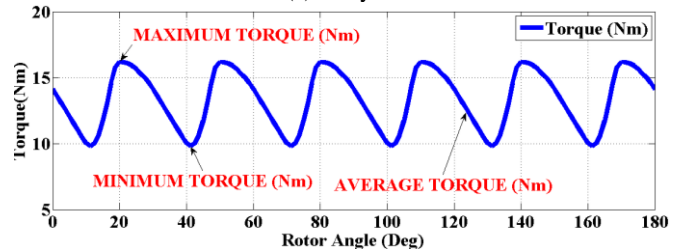
Figure 7: Torque waveform for SyRM with round barrier

Figure 8(a) infers the torque waveform produced by the Synchronous Reluctance motor with three round barriers with notch having maximum, minimum and average Torque values of 14.914 Nm, 8.248 Nm, 11.769 Nm. Therefore, the torque ripple can be calculated by using Expression (25) and the value of torque ripple is 0.566.

Figure 8(b) infers the torque waveform produced by the synchronous reluctance motor with one round barriers with notch having maximum, minimum and average torque values of 16.179 Nm, 9.787 Nm, 13.321 Nm. The Instantaneous Fields of SyRM with notch and angled barrier.



(a). 3 layers



(b). 1 layer

Figure 8: Torque waveform of SyRM with notch and round barrier

Figure 9 depicts the instantaneous fields distributed in the Synchronous Reluctance motor with notch and angled barrier having maximum flux density of 2.22 Tesla.

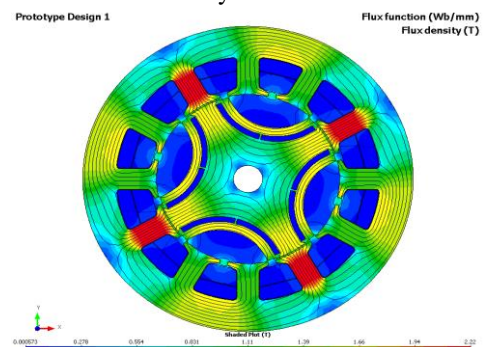


Figure 9: Instantaneous Fields of SyRM with notch and angled barrier (1-layer)

Table 1: Torque developed by SyRM with angled barrier for different layers

Layer Torque	1 layer	2 layers	3 layers	4 layers
Minimum torque	1.426	8.909	10.136	1.449
Maximum torque	22.84	16.221	18.424	24.299
Average torque	11.831	12.285	13.968	11.827
Torque ripple	1.81	0.595	0.593	1.931

Table 2: Torque developed by SyRM with notch and angled barrier for different layers

Layer Torque	1 layer	2 layers	3 layers	4 layers
Minimum torque	5.361	6.821	1.671	4.618
Maximum torque	17.377	21.110	24.770	16.176
Average torque	13.055	12.481	13.702	11.594
Torque ripple	0.92	1.144	1.685	0.987

Table 3: Torque developed by SyRM with round barrier for different layers

Layer Torque	1 layer	2 layers	3 layers	4 layers
Minimum torque	7.970	7.082	7.684	7.298
Maximum torque	14.698	17.907	17.596	17.277
Average torque	11.069	12.117	11.439	11.842
Torque ripple	0.607	0.843	0.918	0.842

Table 4: Torque developed by SyRM with notch and round barrier for different layers

Layer Torque	1 layer	2 layers	3 layers	4 layers
Minimum torque	9.787	1.952	8.248	8.477
Maximum torque	16.179	20.155	14.914	16.422
Average torque	13.321	12.422	11.769	12.135
Torque ripple	0.497	1.494	0.566	0.656

From the FEA findings shown in *table 1*, *table 2*, *table 3* and *table 4*, it is observed that Synchronous reluctance motor with notch and round barrier rotor specifically layer 1 is having maximum value of average torque and the torque ripple for the motor is very less when compared to other variations of Synchronous reluctance motors. Therefore, Synchronous reluctance motor with notch and round barrier having one layer is found to be best for the EV applications.

4. CONCLUSION

This research article presents a modified synchronous reluctance motor for electrical drive. The detailed mathematical analysis of designing the SyRM is also presented. The various designs of SyRM in terms of its rib structure and flux barrier are analyzed in order to achieve low torque ripple without affecting the average torque of the motor in electromagnetic domain and dimensions of the basic motor. From the FEA findings, it is clear that Synchronous reluctance motor with notch and round barrier having one layer design has lower torque ripple and also provides maximum torque values, leads to low acoustic noise which is best suitable for EV applications. In future, this research is extendable in predicting the temperature rise analysis and selection of laminating core material with its verification in laboratory arrangement.

REFERENCES

- [1] Kumar, Busireddy Hemanth.; and Vivekanandan Subburaj. Integration of RES with MPPT by SVPWM Scheme. Intelligent Renewable Energy Systems. 2022; 157-178. <https://doi.org/10.1002/9781119786306.ch6>
- [2] Hemanth Kumar, B.; A. Bhavan.; C. V. Jeevithesh.; Sanjeevikumar Padmanab.; and Vivekanandan Subburaj. A New Series-Parallel Switched Capacitor Configuration of a DC-DC Converter for Variable Voltage Applications. In Electric Vehicles: Springer, Singapore, 2021; pp. 247-270. https://doi.org/10.1007/978-981-15-9251-5_15
- [3] B. Hemanth Kumar, S. Prabhu, K. Janardhan, V. Arun and S. Vivekanandan. A Switched Capacitor-Based Multilevel Boost Inverter for Photovoltaic Applications. Journal of Circuits, Systems and Computers. <https://doi.org/10.1142/S0218126623500573>
- [4] Wu, G.; Huang, S.; Wu, Q.; Rong, F.; Zhang, C.; Liao, W. Robust predictive torque control of N*3-phase PMSM for high-power traction application. IEEE Trans. Power Electron. 2020, 35, 10799–10809. DOI: 10.1109/TPEL.2020.2981914
- [5] Taghavi, S.; Pillay, P. A sizing methodology of the synchronous reluctance motor for traction applications. IEEE J. Emerg. Sel. Top. Power Electron. 2014, 2, 329–340. DOI: 10.1109/JESTPE.2014.2299235
- [6] Moghaddam, R.R.; Magnussen, F.; Sadarangani, C. Theoretical and experimental reevaluation of synchronous reluctance machine. IEEE Trans. Ind. Electron. 2010, 57, 6–13. DOI: 10.1109/TIE.2009.2025286
- [7] Bianchi, N.; Fornasiero, E.; Soong, W. Selection of PM flux linkage for maximum low-speed torque rating in a PM-assisted synchronous reluctance machine. IEEE Trans. Ind. Appl. 2015, 51, 3600–3608. DOI: 10.1109/TIA.2015.2416236
- [8] Di Nardo, M.; Calzo, G.L.; Galea, M.; Gerada, C. Design optimization of a high-speed synchronous reluctance machine. IEEE Trans. Ind. Appl. 2018, 54, 233–243. DOI: 10.1109/TIA.2017.2758759
- [9] Boldea, I. Control issues in adjustable speed drives. IEEE Ind. Electron. Mag. 2008, 2, 32–50. DOI: 10.1109/MIE.2008.928605
- [10] Betz, R.; Lagerquist, R.; Jovanovic, M.; Miller, T.; Middleton, R. Control of synchronous reluctance machines. IEEE Trans. Ind. Appl. 1993, 29, 1110–1122. DOI: 10.1109/28.259721
- [11] Wang, Y.; Ionel, D.M.; Dorrell, D.G.; Stretz, S. Establishing the power factor limitations for synchronous reluctance machines. IEEE Trans. Magn. 2015, 51, 1–4. DOI: 10.1109/TMAG.2015.2443713
- [12] Vagati, A.; Canova, A.; Chiampi, M.; Pastorelli, M.; Repetto, M. Design refinement of synchronous reluctance motors through finite-element analysis. IEEE Trans. Ind. Appl. 2000, 36, 1094–1102. DOI: 10.1109/28.855965
- [13] Park, J.-M.; Park, S.-J.; Lee, M.-M.; Chun, J.-S.; Lee, J.-H. Rotor design on torque ripple reduction for a synchronous reluctance motor with concentrated winding using response surface methodology. IEEE Trans. Magn. 2006, 42, 3479–3481. DOI: 10.1109/TMAG.2006.879501
- [14] Bianchi, N.; Bolognani, S.; Bon, D.; Pr, M.D. Torque harmonic compensation in a synchronous reluctance motor. IEEE Trans. Energy Convers. 2008, 23, 466–473. DOI: 10.1109/TEC.2007.914357

- [15] Diao, X.; Zhu, H.; Qin, Y.; Hua, Y. Torque ripple minimization for bearingless synchronous reluctance motor. *IEEE Trans. Appl. Supercond.* 2018, 28, 1–5. DOI: 10.1109/TASC.2018.2798632
- [16] S. Prabhu and M. Balaji, "Performance Analysis of Permanent Magnet Assisted Outer Rotor Switched Reluctance Motor with Non-Oriented Laminating Material for Electric Transportation Systems," 2022 IEEE 2nd International Conference on Sustainable Energy and Future Electric Transportation (SeFeT), 2022, 1-6. DOI: 10.1109/SeFeT55524.2022.9909350.
- [17] Sundaramoorthy Prabhu., M., B., K., S., Natesan, E. and K., M. Vibration analysis of E-core flux reversal free stator switched reluctance motor. *Circuit World*. 2020, 46, 325-334. DOI: 10.1108/CW-09-2019-0116.
- [18] Sivasamy, S., Maria, M.M.B. and Sundaramoorthy, P., 2021. Performance investigation of doubly salient outer rotor switched reluctance motor using finite element analysis. *Circuit World*, 2020. <https://doi.org/10.1108/CW-06-2020-0115>



© 2022 by Busireddy Hemanth Kumar, Deepak Prakash Kadam, Saka Rajitha, Prabhu Sundaramoorthy, T. Penchalaiah and Kavali Janardhan. Submitted for possible open access publication under the terms and conditions of the Creative Commons Attribution (CC BY) license (<http://creativecommons.org/licenses/by/4.0/>).